

Structural characteristics and physicochemical properties of oxidized corn starches varying in amylose content

Daris Kuakpetoon and Ya-Jane Wang*

Department of Food Science, University of Arkansas, 2650 N. Young Ave., Fayetteville, AR 72704, USA

Received 23 January 2006; received in revised form 23 March 2006; accepted 6 April 2006

Available online 11 May 2006

Abstract—The effects of amylose content on the extent of oxidation and the distribution of carboxyl groups in hypochlorite-oxidized corn starches were investigated. Corn starches including waxy corn starch (WC), common corn starch (CC), and 50% and 70% high-amylose corn starches (AMC) were oxidized with NaOCl at three concentrations (0.8%, 2%, and 5%). Carboxyl and carbonyl content of oxidized starches increased with increasing NaOCl concentration. High-AMC (70%) had slightly higher carboxyl and carbonyl contents at 0.8% NaOCl, whereas WC had significantly higher carboxyl and carbonyl contents at 2% and 5% NaOCl levels. Carbohydrate profiles by high-performance size-exclusion chromatography indicate that amylose was more susceptible to depolymerization than amylopectin. Degradation of amylopectin long chains ($DP > 24$) was more pronounced in WC and CC than in AMCs. The crystalline lamellae of WC started to degrade at 2% NaOCl, but those of the other corn starches remained intact even at 5% NaOCl level according to X-ray crystallinity. By using anion-exchange chromatography for separation and size-exclusion chromatography for characterization, carboxyl groups were found to be more concentrated on amylopectin than on amylose, particularly in AMCs. Oxidation decreased gelatinization temperature and enthalpy with WC showing the most decrease and 70% AMC showing the least. The gelatinization enthalpy of 50% AMC decreased significantly faster than those of CC and 70% AMC after 0.8% oxidation. Retrogradation of amylopectin slightly increased after oxidation with increasing oxidation level. The peak viscosities of oxidized WC and CC were higher than those of their native counterparts at 0.8% NaOCl, but this increase was not observed in AMCs. The setback viscosities of 2% NaOCl-oxidized 50% and 70% AMCs were much higher than those of the unmodified counterparts. The extent of oxidation and physicochemical properties of oxidized starches varied greatly with the amylose:amylopectin ratio of corn starches. Amylose was suggested to play an important role in controlling the oxidation efficiency. © 2006 Elsevier Ltd. All rights reserved.

Keywords: Hypochlorite-oxidized starch; Carboxyl; Carbonyl; Amylopectin chain length distribution; Starch structure; High-amylose corn starch

1. Introduction

Oxidized starch has been widely used in many industries, particularly the paper, textile, laundry finishing, and building materials industries to provide surface sizing and coating properties.¹ Oxidized starch also becomes increasingly important in the food industry for its unique functional properties such as low viscosity, high stability, clarity, film forming, and binding properties. Oxidized starch can be used as a coating and sealing agent in confectionary, as an emulsifier,² as a dough

conditioner for bread,³ as a gum arabic replacer,⁴ and as a binding agent in batter applications.

Most oxidized starch for food applications is produced by reacting starch with a specified amount of sodium hypochlorite (NaOCl) under controlled temperature and pH.⁵ Two main reactions occur during oxidation. Firstly, starch hydroxyl groups are oxidized to carbonyl groups and then to carboxyl groups. This reaction primarily takes place on the hydroxyl groups at the C-2, C-3, and C-6 positions.⁵ Secondly, oxidation also causes degradation of starch molecules by mainly cleaving amylose and amylopectin molecules at α -1,4 glucosidic linkages.⁵ Therefore, the carboxyl and carbonyl contents and the degree of depolymerization in oxidized starch are indicators of the degree of oxidation.

* Corresponding author. Tel.: +1 479 575 3871; fax: +1 479 575 6936; e-mail: yjwang@uark.edu

The extent of oxidation can be affected by many factors, including pH, temperature, hypochlorite concentration, starch molecular structure, and starch source.⁵ Many studies have reported that starch source and structure highly influenced the extent of oxidation.^{6–11} Recent results by Kuakpetoon and Wang¹² showed that potato starch was much more prone to oxidation than were corn and rice starches under the same oxidation conditions. Potato starch displays the B-type X-ray diffraction pattern, which has a looser crystalline arrangement and a lower crystallinity compared with A-type starches.^{13,14} Therefore, starches containing more loosely packed crystalline structure or more amorphous structure may provide more accessible reaction sites for the oxidizing agent. Any chemical characteristics affecting the packing of crystalline lamellae and the size of amorphous lamellae could also influence the extent of oxidation. Starches with short average chain lengths display A-type crystalline patterns, and long and intermediate average chain lengths are associated with B-type and C-type crystalline patterns, respectively.^{15,16} Although potato and high-amylose corn starches exhibit a similar B-type crystalline polymorphism, high-amylose corn starches may show different oxidation efficiency when compared to potato starch because of their high amylose contents. Jenkins and Donald¹⁷ investigated the influence of amylose on corn starch granule structure using small-angle X-ray scattering (SAXS) and observed that the combined size of the crystalline and amorphous lamellae was constant at 9 nm for all three corn starches varying in amylose content (0%, 28%, and 70%). However, the size of the amorphous lamellae decreased with increasing amylose content. They suggested that amylose might disrupt the packing of amylopectin double helices by co-crystallizing with amylopectin chains and pulling some amylopectin chains from two adjacent crystalline lamellae closer to each other. Therefore, the amount of amylose may also affect the access of oxidizing agent to starch during oxidation.

The objectives of this study were to investigate the influence of amylose content on the extent of oxidation and on the distribution of carboxyl groups in corn starches with different amylose contents, including waxy, common, 50%, and 70% high-amylose corn starches. The physicochemical properties of the oxidized starches were also determined and compared.

2. Results and discussion

2.1. Carbonyl and carboxyl contents

Both carboxyl and carbonyl contents of the oxidized corn starches increased with increasing hypochlorite concentration (Table 1), agreeing with previous reports.^{11,12,18–20} Carboxyl content increased at a much faster rate than carbonyl content, which confirmed that hydroxyl groups on starch molecules were initially oxidized to carbonyl groups and then to carboxyl groups as the primary final product. The corn starches, regardless of their amylose contents, were similar in their carbonyl and carboxyl contents at 0.8% NaOCl. When NaOCl level was increased to 2% and 5%, waxy corn starch (WC) had the highest carboxyl group, and 70% high-amylose corn starch (AMC) had the lowest. It is speculated that the production of carboxyl groups on starch molecules was hindered by the increased amount of amylose in 70% AMC. Kuakpetoon and Wang¹² investigated the X-ray diffraction patterns of oxidized rice, common corn, and potato starches at 0.8 and 2% NaOCl levels, and found that there were no significant changes in their crystallinity after oxidation. They concluded that the oxidation mainly took place in the amorphous lamellae rather than in the crystalline lamellae. By using small-angle X-ray scattering (SAXS), Jenkins and Donald¹⁷ measured the size of amorphous lamellae of corn starch varying in amylose content and reported that the size of the amorphous lamellae of 70% AMC was smaller than that of CC. Therefore, 70% AMC would have much less accessible area for NaOCl and water molecules to form a carboxyl group compared with WC and CC. However, 50% AMC contained a significantly larger number of carbonyl and carboxyl groups than common corn starch (CC) at 5% NaOCl. These results imply that the size of the amorphous lamellae in 50% AMC might not be the sole factor in determining the extent of oxidation.

2.2. Degradation of starch from oxidation

The normalized HPSEC chromatograms of unmodified and oxidized corn starches are presented in Figure 1. WC consists of only amylopectin; therefore, the carbohydrate profile of WC (Fig. 1A) can illustrate the effect

Table 1. Carbonyl and carboxyl content (% db) of oxidized starches

Starch	0.8% NaOCl		2% NaOCl		5% NaOCl	
	Carbonyl	Carboxyl	Carbonyl	Carboxyl	Carbonyl	Carboxyl
Waxy corn	0.02 ^b	0.03 ^{b1}	0.07 ^a	0.18 ^a	0.17 ^a	0.76 ^a
Common corn	0.02 ^b	0.03 ^b	0.05 ^b	0.16 ^b	0.11 ^d	0.56 ^c
50% Amylose corn	0.03 ^b	0.03 ^b	0.05 ^b	0.14 ^b	0.14 ^b	0.65 ^b
70% Amylose corn	0.05 ^a	0.04 ^a	0.06 ^{ab}	0.08 ^c	0.13 ^c	0.48 ^d

Means of duplicate measurements in the same column followed by the same letter are not significantly different at the 95% confidence level.

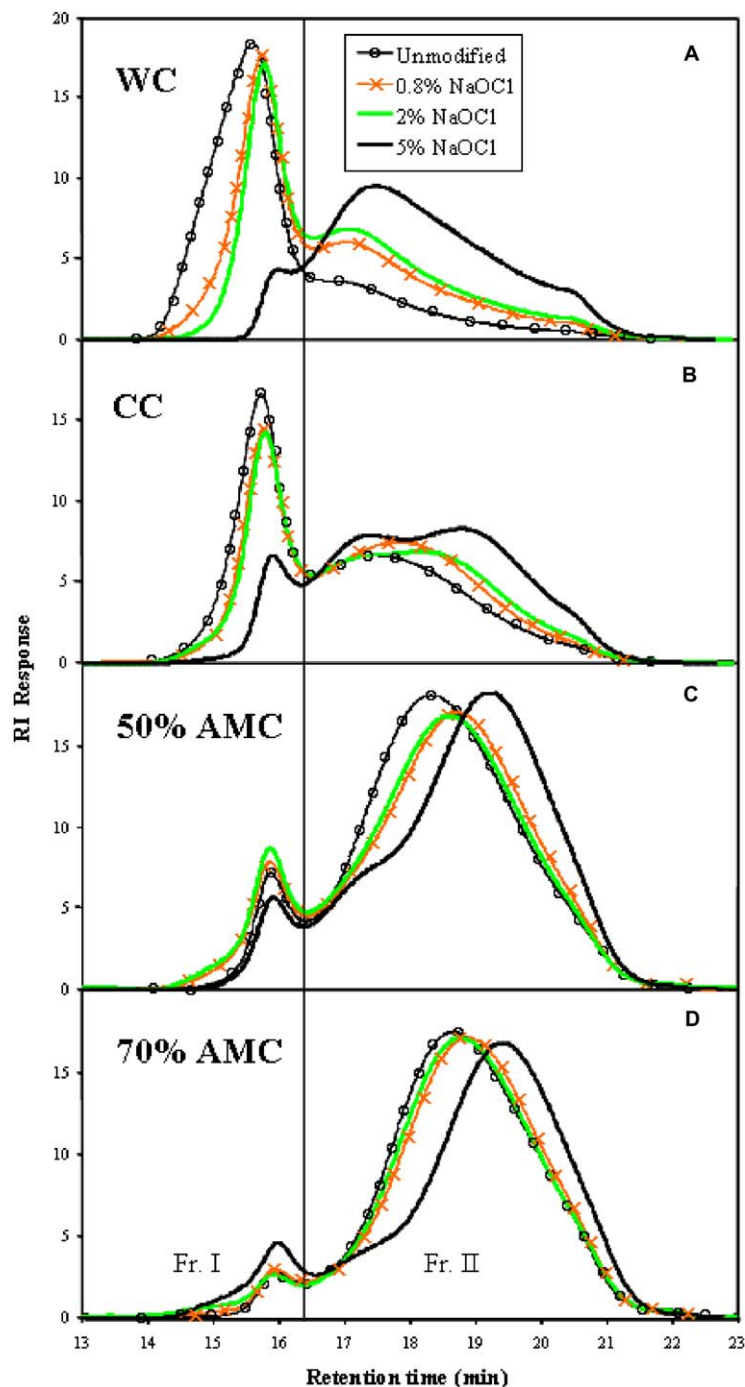


Figure 1. Normalized high-performance size-exclusion chromatograms of unmodified and hypochlorite-oxidized starches. (A) WC = waxy corn starch; (B) CC = common corn starch; (C) 50% AMC = 50% amylose corn starch, and (D) 70% AMC = 70% amylose corn starch.

of hypochlorite oxidization on degradation of amylopectin and amylose when compared with those of other starches. WC displayed a bimodal distribution: Fraction I (Fr. I) and Fraction II (Fr. II). Fr. I eluted before 16.3 min consisted of high-molecular-weight (MW) amylopectin (H-AP). Fr. II eluted after 16.3 min comprised low-MW amylopectin (L-AP). The amylose was eluted after 16.3 min and mixed with L-AP according to the chromatograms

of CC, 50% AMC, and 70% AMC (Fig. 1B–D). The H-AP fraction in WC readily degraded into low-MW amylopectin with the peak shifting from 15.5 to 15.9 min at 0.8% NaOCl. The H-AP of WC continued to degrade further when NaOCl concentration increased to 2% and 5% as evidenced by the increased proportion of L-AP fractions. When the amylose content in corn starches increased, the extent of H-AP degradation decreased.

The normalized HPSEC chromatograms of isoamylase-debranched unmodified and oxidized corn starches are shown in Figure 2. Each chromatogram can be divided into three fractions: Fr. I consisted of amylose molecules, Fr. II consisted of AP long B chains, and Fr. III consisted of AP short B chains and A chains. For oxidized starches, Fr. II and Fr. III could also

contain some degraded amylose. Amylose was also degraded during oxidation, and amylose degradation increased with increasing NaOCl level. At low levels of NaOCl such as 0.8%, oxidation was probably only limited by the amount of NaOCl. When NaOCl was increased, the smaller amorphous lamellae in 70% AMCs probably limited the extent of oxidation as

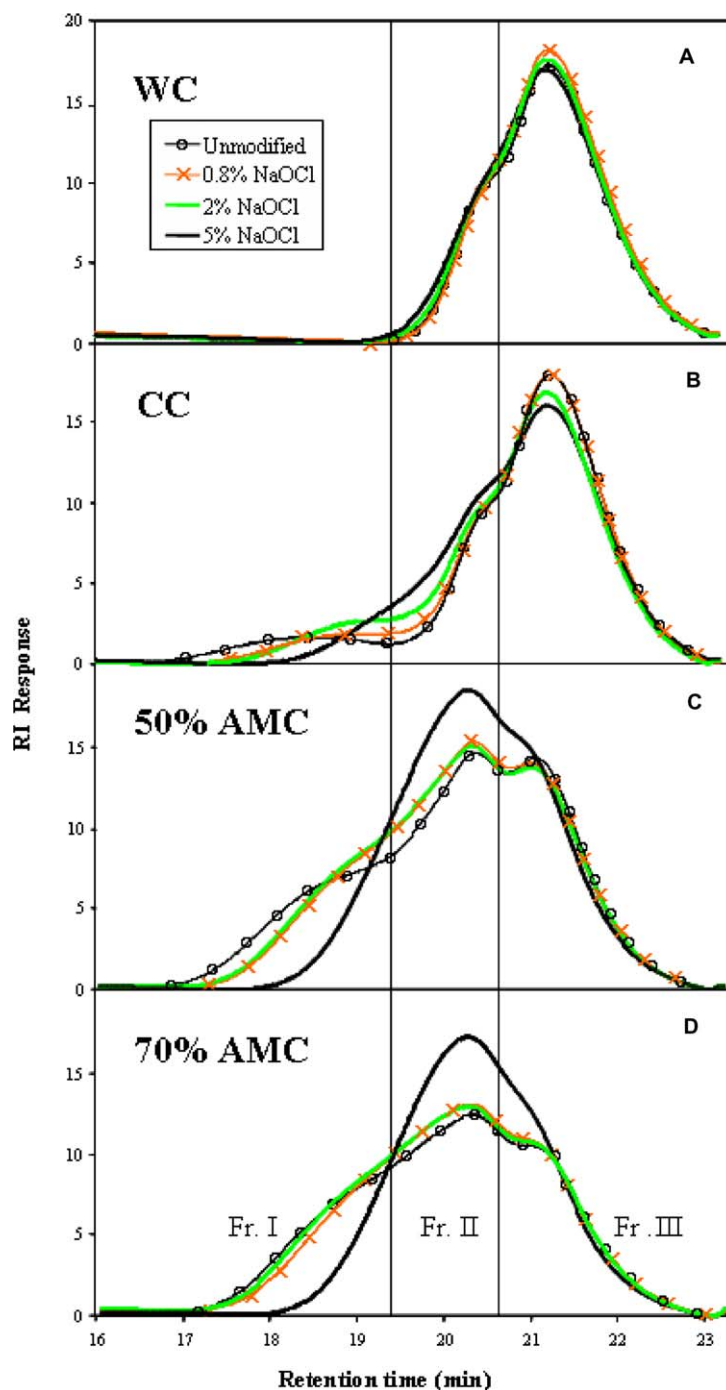


Figure 2. Normalized high-performance size-exclusion chromatograms of isoamylase-debranched unmodified and hypochlorite-oxidized starches. (A) WC = waxy corn starch; (B) CC = common corn starch; (C) 50% AMC = 50% amylose corn starch, and (D) 70% AMC = 70% amylose corn starch.

shown by its lower carboxyl content (Table 1) and less amylose and amylopectin degradation. Oxidized CC showed extensive degradation in amylose and amylopectin at 5% NaOCl (Figs. 1B and 2B), which might explain its lower carboxyl content than 50% AMC. More NaOCl might be consumed for depolymerization of amylose and amylopectin in CC and less NaOCl for the formation of carboxyl groups (Table 1).

The results from Figures 1 and 2 suggest that amylose was more prone to depolymerization than was amylopectin at the same NaOCl level. The H-AP peak in CC did not shift (Fig. 1B), but its amylose peak shifted from 18.1 to 18.6 min (Fig. 2B); the H-AP peak in WC shifted from 15.5 to 15.9 min at 0.8% NaOCl oxidation. The difference in susceptibility to NaOCl degradation between amylose and amylopectin may explain the lesser amount of degradation of the H-AP fraction with increasing amylose content. Amylose might more readily react with NaOCl, and thereafter, less NaOCl was available for the oxidation of amylopectin. It is speculated that the linear chemical structure or the random arrangement of amylose makes amylose more susceptible to oxidative degradation.

The results also show that the degradation of amylopectin and amylose was not proportional to the level of NaOCl for different corn starches. Significant changes in amylopectin and amylose fractions were observed between 0% and 0.8% NaOCl and between 2% and 5% NaOCl, but the chromatograms of 0.8% and 2% NaOCl were very similar (Figs. 1 and 2). This non-linear relationship was also noted for the change in carboxyl content (Table 1). These results imply that there might be two locations within starch granules with different acces-

sibility or susceptibility to oxidation. The first rapid degradation at 0.8% NaOCl should occur in the amorphous lamellae where NaOCl was easy to access and react with amylopectin and amylose. When NaOCl concentration was increased from 0.8% to 2%, NaOCl may begin to penetrate into and oxidize the crystalline lamellae, which explained the slower degradation rate from 0.8% to 2% NaOCl. After the crystalline lamella was attacked and probably became exposed, the rapid oxidation rate resumed when NaOCl was increased to 5%.

The change in amylopectin chain-length distribution from oxidation was further elucidated using HPAEC-PAD (Table 2 and Fig. 3). AP branches were grouped into four chain types; namely, A, B1, B2, and B3+ chains corresponding to their chain length of degree of polymerization (DP) 6–12, 13–24, 25–36, and >37, respectively, according to Hanashiro et al.²¹ The average chain length can be used to indicate the degradation of AP. Similar to the HPSEC results (Figs. 1 and 2), the AP of WC and CC degraded at a slightly faster rate than those of 50% and 70% AMCs according to their changes in average chain length.

According to the revised cluster model of AP proposed by Hizukuri,²² A and B1 chains are located within a single cluster in which they form double helices, which corresponds to one crystalline lamella, whereas B2 and B3+ chains extend through two or more clusters. Therefore, B2 and longer chains are present in both the crystalline and amorphous lamellae. Based on this model, the degradation of each chain type after oxidation could indirectly suggest the site of oxidation. The percentages of B2 and B3+ chains in WC and CC decreased with increasing NaOCl concentration, while those of A and

Table 2. Chain-length distribution of amylopectins of isoamylase-debranched unmodified and hypochlorite-oxidized corn starches by HPAEC-PAD^a

Starch	Oxidation level (% NaOCl)	Average chain length (DP)	% Chain-length distribution			
			A chain (DP 6–12)	B1 chain (DP 13–24)	B2 chain (DP 25–36)	B3+ chains (DP ≥37)
Waxy corn	Unmodified	20.69 ± 0.08	24.2 ± 0.0	49.9 ± 0.2	15.3 ± 0.1	10.6 ± 0.3
	0.8	20.71 ± 0.06	24.2 ± 0.2	49.8 ± 0.1	15.3 ± 0.3	10.6 ± 0.2
	2	20.42 ± 0.07	24.8 ± 0.3	50.4 ± 0.3	14.9 ± 0.3	10.0 ± 0.2
	5	18.91 ± 0.07	27.2 ± 0.1	51.8 ± 0.4	14.8 ± 0.4	6.3 ± 0.1
Common corn	Unmodified	20.64 ± 0.09	24.4 ± 0.7	50.3 ± 0.6	14.7 ± 0.1	10.7 ± 0.2
	0.8	20.56 ± 0.03	24.4 ± 0.0	50.6 ± 0.1	14.5 ± 0.0	10.5 ± 0.1
	2	20.09 ± 0.17	25.5 ± 0.2	50.8 ± 0.7	14.3 ± 0.2	9.4 ± 0.6
	5	18.97 ± 0.33	28.9 ± 0.1	51.4 ± 0.3	11.9 ± 0.5	7.8 ± 0.5
50% Amylose corn	Unmodified	24.92 ± 0.31	16.3 ± 0.7	45.6 ± 0.7	18.1 ± 0.5	19.9 ± 0.9
	0.8	24.19 ± 0.08	18.0 ± 0.4	46.3 ± 0.9	17.2 ± 0.5	18.6 ± 0.4
	2	24.72 ± 0.04	16.4 ± 0.1	45.8 ± 0.1	18.8 ± 0.1	19.1 ± 0.2
	5	23.92 ± 0.21	17.4 ± 0.6	46.5 ± 0.9	19.2 ± 0.7	17.0 ± 0.4
70% Amylose corn	Unmodified	26.49 ± 0.06	15.1 ± 0.5	42.01 ± 0.9	18.7 ± 0.4	24.2 ± 0.7
	0.8	25.74 ± 0.23	15.7 ± 0.2	42.27 ± 0.6	20.5 ± 0.1	21.5 ± 0.7
	2	25.28 ± 0.08	16.2 ± 0.9	41.42 ± 0.5	21.3 ± 0.5	21.1 ± 0.1
	5	25.06 ± 0.16	15.5 ± 0.3	43.16 ± 0.1	21.7 ± 0.2	19.6 ± 0.3

^a The data were averages of two measurements with standard deviations.

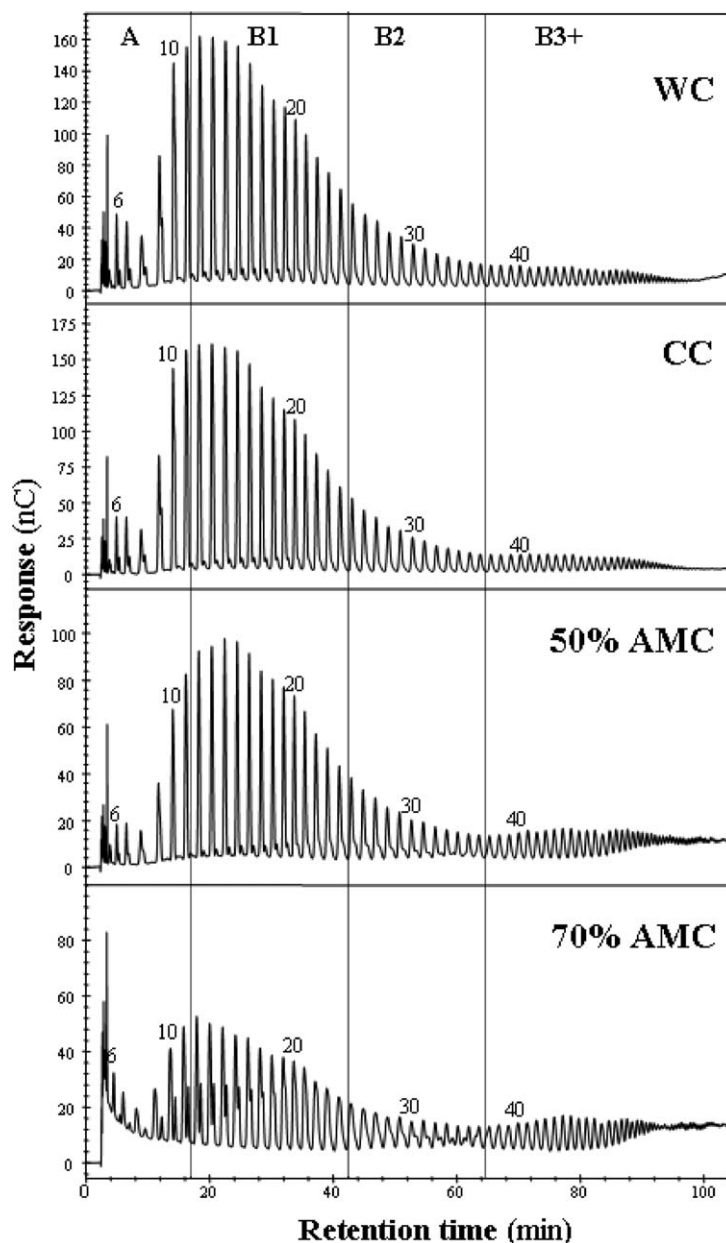


Figure 3. HPAEC–PAD chromatograms of isoamylase-debranched unmodified corn starches. The number above the peak represents its degree of polymerization in glucose units.

B1 chains increased. These results demonstrate that oxidative depolymerization mainly took place in the amorphous lamellae. Nevertheless, depolymerization might also occur to B1 chains in the crystalline lamellae at 5% NaOCl oxidation because of the significant increase of the percentage of A chains in WC and CC. The B2 and B3+ chains decreased slightly more for CC than for WC at 5% NaOCl, which may explain the lower carbonyl and carboxyl contents in CC than those in WC (Table 1). When a large amount of NaOCl was applied, that is, 5%, some NaOCl might be preferentially consumed for the degradation of amylose and amylopectin. Therefore, less NaOCl was available for the formation

of carboxyl or carbonyl groups in CC than in WC. AMCs of 50% and 70% showed a decrease in the percentage of B3+ chains but a slight increase in the other chains. These differences were attributed to the smaller amorphous lamellae in high-amylose corn starches as previously discussed.

2.3. X-ray diffraction

The X-ray diffractograms of native and oxidized corn starches are depicted in Figure 4, and their degrees of crystallinity are summarized in Table 3. WC and CC belong to the A-type, whereas 50% and 70% AMCs belong

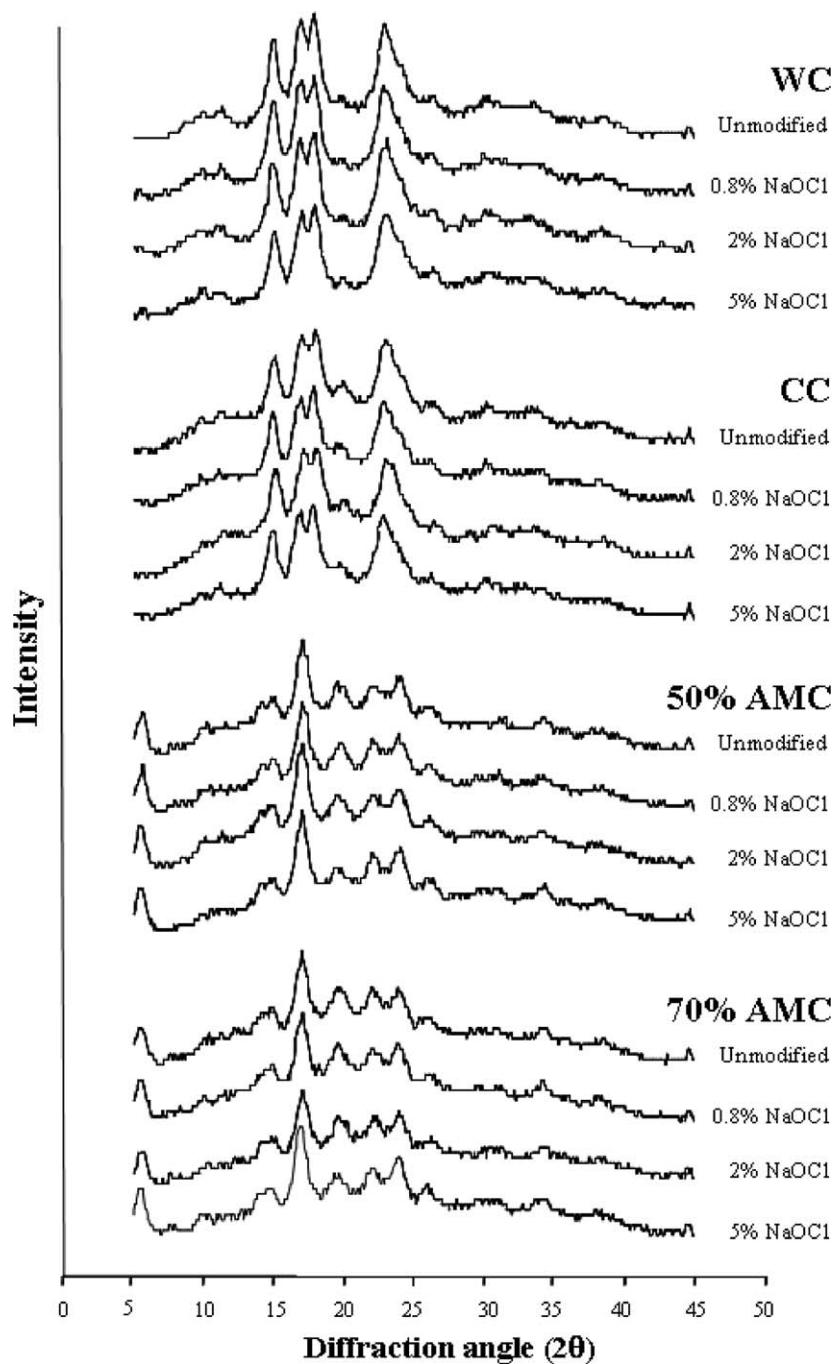


Figure 4. X-ray diffractograms of unmodified and hypochlorite-oxidized corn starches.

Table 3. X-ray crystallinity of unmodified and hypochlorite-oxidized corn starches

Starch	Crystallinity (%)			
	Unmodified	0.8 NaOCl	2 NaOCl	5 NaOCl
Waxy corn	47.9 ^a	50.9 ^b	48.7 ^c	44.7 ^d
Common corn	35.5 ^a	35.2 ^a	28.0 ^b	40.5 ^c
50% Amylose corn	25.4 ^a	28.4 ^b	26.3 ^c	25.7 ^d
70% Amylose corn	26.9 ^a	26.5 ^a	25.4 ^b	34.8 ^c

Means of duplicate measurements in the same row followed by the same letter are not significantly different at the 95% confidence level.

to the B-type X-ray diffraction pattern. Among the unmodified starches WC had the highest crystallinity, while 50% AMC had the lowest, indicating the correlation between crystallinity and the amount of amylopectin B1 chains, because amylopectin B1 chains are mainly responsible for the formation of the crystalline lamellae.¹⁶ It is speculated that amylose, which is the predominant component in 70% AMC, may co-crystallize with each other or with amylopectin long chains, which contributed to a slightly higher crystallinity of 70% AMC over 50% AMC.

The crystallinity of WC increased after 0.8% NaOCl oxidation but decreased when NaOCl was increased to 2% and 5%. This trend supports our previous assumption on the progress of oxidation in WC at different NaOCl concentrations. Starch molecules in the amorphous lamellae were first degraded at 0.8% NaOCl, resulting in an increase in overall crystallinity. When the NaOCl level was increased to 2% and 5%, a portion of the crystalline lamellae in WC was degraded; consequently, its crystallinity decreased. CC and 70% AMC followed a similar pattern of change in crystallinity. At 0.8% NaOCl, most oxidation probably occurred to amylose in the amorphous lamellae; thus little change in crystallinity was observed. When the amorphous lamellae were degraded further at 5% NaOCl, the overall crystallinity increased. The data suggest that little depolymerization occurred in the crystalline lamellae of CC and 70% AMC at 5% NaOCl. The change in crystallinity in 50% AMC was different from that of 70% AMC but more close to that of WC when treated with different NaOCl levels. One possible explanation is that amylose in 50% AMC might be present more in the form of an amylose–lipid complex, whereas amylose in 70% AMC might also form crystalline structure or co-crystallize with amylopectin besides forming amylose–lipid complex. This assumption is supported by the lower crystallinity in unmodified 50% AMC (Table 3) and the greater amylose degradation in oxidized 50% AMC at 0.8% NaOCl (Fig. 2) as compared with those of 70% AMC. After the amylose–lipid complexes in the amorphous regions were degraded at 0.8% NaOCl oxidation, the crystallinity significantly increased. Similar to CC and 70% AMC, the crystalline lamellae of 50% AMC were not significantly degraded at 5% NaOCl (Table 3).

2.4. The distribution of carboxyl groups in oxidized starches

The location of depolymerization from oxidation has been discussed in the previous sections, but those data did not reveal the respective distribution of carboxyl groups on amylose and amylopectin. Zhu et al.²³ fractionated hypochlorite-oxidized potato starch into bound and unbound dextrans by an ion-exchange DEAE-Sepharose column. Based on ¹³C NMR spectroscopy, they

confirmed that only bound dextrans showed the signal assigned to carboxylic carbon at $\delta = 176.0$ and 177.0 ppm. Therefore, DEAE-Sepharose ion-exchange chromatography was employed in this study to fractionate the oxidized corn starches into bound and unbound dextrans. The oxidized corn starches at 0.8% NaOCl were not fractionated in this study due to their very low carboxyl contents. The recovered bound and unbound dextrans were characterized by HPSEC, and their native and isoamylase-debranched profiles are presented in Figures 5 and 6, respectively. The chromatograms of the whole dextrans were between those of their unbound and bound dextrans, indicating that the ion-exchange separation condition did not alter the structure of the starch molecules. The unbound dextrans were degraded to a greater extent than the bound dextrans for all oxidized starches at both 2% and 5% NaOCl levels (Fig. 5). The bound dextrans consisted of a larger proportion of H-AP (Fr. I) than the unbound dextrans, and the H-AP of the unbound dextrans almost disappeared after 5% NaOCl oxidation. The isoamylase-debranched unbound dextrans displayed a monodisperse profile for all starches at 5% NaOCl level. This implies that the unbound dextrans from 5% NaOCl oxidation consisted of highly degraded fragments because probably most of the amorphous lamellae were degraded at 5% NaOCl. At 2% NaOCl level, some amylose and amylopectin long chains were not degraded; thus the unbound dextrans displayed the bimodal distribution. The formation of carboxyl groups might occur at different locations from where the degradation took place. Therefore, the bound and unbound dextrans showed different extents of degradation.

The amylopectin structures of the bound and unbound dextrans from oxidized WC were further examined by HPAEC–PAD (Table 4). Because of the limited sample size, amylose was not separated from the unbound and bound dextrans; therefore, the data in Table 4 are slightly different from those in Table 2. Nevertheless, the data were valid for comparison among the different oxidation levels for the same starch. At 2% NaOCl level, where most oxidation occurred to the amorphous lamellae or slightly penetrating into the crystalline lamellae, the bound dextrans contained a much larger proportion of A chains but a smaller proportion of B3+ chains than the unbound dextrans. This implies that the degradation at 2% NaOCl took place mainly on B2 and B3+ chains in the amorphous lamellae. The unbound WC dextrans had a similar chain-length distribution as the whole one at 2% NaOCl. When WC was oxidized at 5% NaOCl, oxidation took place in the crystalline lamellae in addition to the amorphous lamellae. At this level, the unbound dextrans contained a much larger number of A chains and a significantly smaller number of B2 and B3+ chains than the whole distribution. It can be concluded that oxidation first degraded

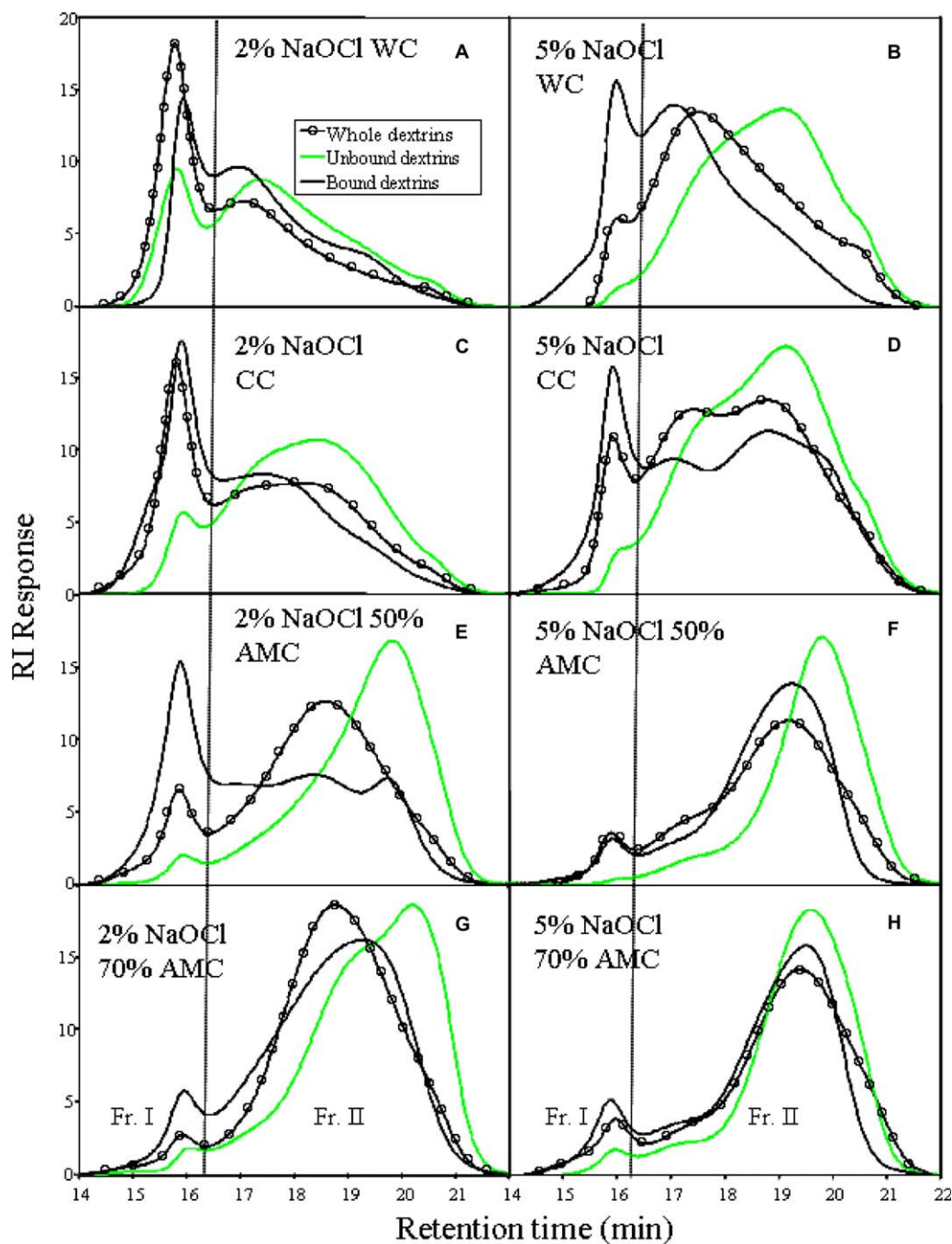


Figure 5. Normalized high-performance size-exclusion chromatograms of whole, unbound, and bound dextrins of 2% and 5% hypochlorite-oxidized corn starches.

B2 and B3+ chains in the amorphous lamellae. The chain-length distribution in the bound dextrins at 5% NaOCl was close to that of the bound dextrins at 2% NaOCl. This confirms that the carboxyl group might be formed at different locations from where the degradation occurred. Based on beta-amylolysis results, Zhu et al.²³ concluded that carboxyl formation was either close to the non-reducing end or toward the reducing end in hypochlorite-oxidized potato starch. The carboxyl formation might take place close to the branching

points of A and B1 chains because oxidation mostly occurred in the amorphous lamellae where the branching points are located.

Oxidized CC, 50% AMC, and 70% AMC starches followed a similar pattern of carboxyl formation and structure degradation as in oxidized WC. However, some differences were noted in terms of the amount, location, and rate of carboxyl formation, and these differences could be attributed to the influence from amylose. The bound dextrins of 2% NaOCl oxidized 50% and 70%

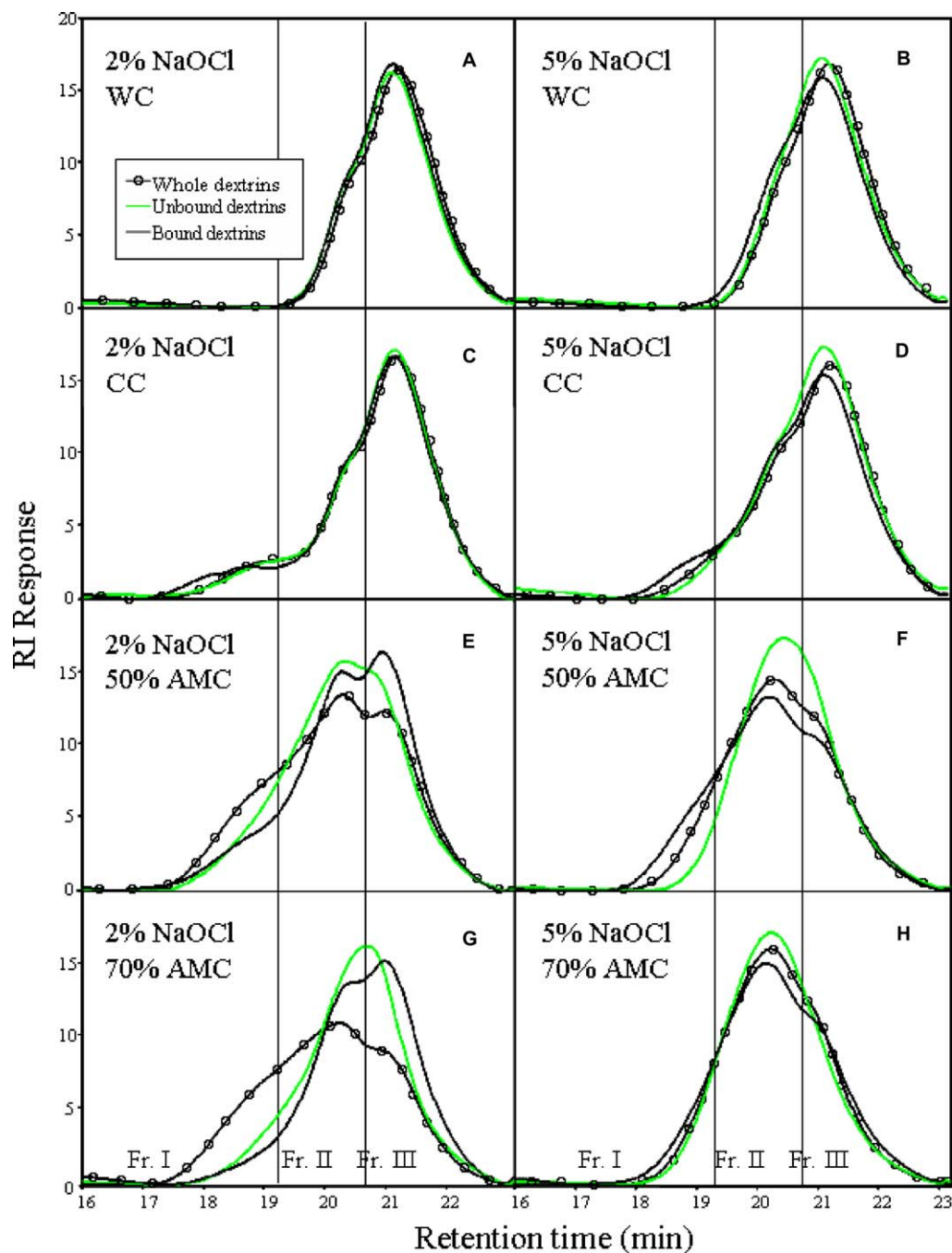


Figure 6. Normalized high-performance size-exclusion chromatograms of isoamylase-debranched whole, unbound, and bound dextrans of 2% and 5% hypochlorite-oxidized corn starches.

AMCs containing a smaller proportion of amylose but a greater proportion of amylopectin than those in the whole and unbound dextrans (Fig. 6E and G). These data infer that the amylose in 50% and 70% AMC seemed to be less susceptible to carboxyl formation but more prone to degradation.

The chain-length distribution of amylopectin in the bound dextrans of oxidized CC, and 50% and 70% AMCs also followed the same pattern as in oxidized

WC. The proportion of A chains increased and that of B chains decreased in bound dextrans, and these changes became more significant at 5% NaOCl. These results support the previous findings that amylose in the amorphous lamellae was preferentially depolymerized before oxidation of amylopectin. Amylopectin might be protected from oxidation by the surrounding amylose molecules or amylose–lipid complexes in the amorphous lamellae.

Table 4. Chain-length distribution of isoamylase-debranched whole, unbound, and bound dextrins of 2% and 5% hypochlorite-oxidized corn starches by HPAEC–PAD^a

Starch	% NaOCl	Fraction	Average chain length (DP)	% Chain length distribution			
				A chain (DP 6–12)	B1 chain (DP 13–24)	B2 chain (DP 25–36)	B3+ chains (DP ≥37)
Waxy corn	2	Whole	20.01 ± 0.10	24.9 ± 0.2	51.9 ± 0.4	14.3 ± 0.4	9.0 ± 0.2
		Bound	19.23 ± 0.10	28.2 ± 0.9	49.9 ± 1.0	14.3 ± 0.3	7.7 ± 0.2
		Unbound	20.05 ± 0.08	25.0 ± 0.1	51.5 ± 0.2	14.4 ± 0.1	9.1 ± 0.3
	5	Whole	18.41 ± 0.07	28.3 ± 0.6	53.2 ± 0.1	12.9 ± 1.0	5.6 ± 0.4
		Bound	18.49 ± 0.13	30.0 ± 1.1	50.7 ± 1.3	13.0 ± 0.5	6.3 ± 0.3
		Unbound	17.73 ± 0.37	31.8 ± 0.9	51.6 ± 1.0	11.4 ± 1.9	5.2 ± 0.1
Common corn	2	Whole	19.49 ± 0.19	26.0 ± 1.1	52.6 ± 0.6	13.3 ± 0.3	8.2 ± 0.3
		Bound	19.26 ± 0.35	27.7 ± 0.7	50.5 ± 0.8	14.2 ± 0.8	7.7 ± 0.7
		Unbound	18.99 ± 0.17	28.0 ± 0.9	51.7 ± 0.4	13.0 ± 0.4	7.4 ± 0.2
	5	Whole	18.54 ± 0.23	27.9 ± 0.5	54.2 ± 0.4	11.4 ± 0.5	6.6 ± 0.4
		Bound	18.02 ± 0.03	32.9 ± 0.2	48.7 ± 0.4	12.1 ± 0.2	6.2 ± 0.1
		Unbound	18.44 ± 0.13	29.6 ± 0.9	51.9 ± 1.4	12.0 ± 1.2	6.6 ± 0.3
50% Amylose corn	2	Whole	22.96 ± 0.16	17.3 ± 0.3	50.9 ± 0.6	17.1 ± 0.6	14.7 ± 0.4
		Bound	21.74 ± 0.57	21.3 ± 0.4	49.2 ± 1.2	17.2 ± 0.2	12.2 ± 1.7
		Unbound	22.83 ± 0.59	20.5 ± 0.6	45.6 ± 0.7	19.2 ± 0.8	14.7 ± 1.8
	5	Whole	23.59 ± 0.10	16.7 ± 0.3	48.9 ± 0.2	18.7 ± 0.5	15.8 ± 0.4
		Bound	20.51 ± 0.06	27.2 ± 1.8	46.5 ± 0.6	15.2 ± 0.3	11.1 ± 0.5
		Unbound	23.10 ± 0.16	21.4 ± 1.4	41.7 ± 0.7	22.1 ± 1.9	14.8 ± 1.2
70% Amylose corn	2	Whole	22.93 ± 0.14	16.9 ± 0.1	50.5 ± 0.5	18.0 ± 0.6	14.6 ± 0.2
		Bound	21.59 ± 0.01	22.7 ± 1.4	47.6 ± 1.5	17.5 ± 0.4	12.2 ± 0.6
		Unbound	23.22 ± 0.17	21.6 ± 0.8	41.1 ± 0.4	22.0 ± 1.9	15.4 ± 1.3
	5	Whole	23.6 ± 0.29	16.0 ± 1.0	47.8 ± 0.1	20.5 ± 0.3	15.7 ± 0.7
		Bound	21.01 ± 0.24	26.2 ± 0.7	45.6 ± 1.0	16.1 ± 1.2	12.1 ± 1.5
		Unbound	23.90 ± 0.67	20.0 ± 0.9	41.0 ± 1.1	21.7 ± 0.5	17.4 ± 1.9

^a The data were averages of two measurements with standard deviations.

2.5. Gelatinization properties

Gelatinization properties of unmodified and oxidized corn starches measured by differential scanning calorimetry (DSC) are summarized in Table 5, and their thermograms are presented in Figure 7. The onset gelatinization temperature (T_o) and gelatinization enthalpy (ΔH_g) of all corn starches decreased with increasing NaOCl concentration; however, the changes varied with starch type. Many studies^{24–29} have shown that starch T_o increases when amylopectin has a high percentage of B1 chains (DP 13–24) and a low percentage of A chains (DP 6–12). Both chain types are located in a single crystalline cluster,²² which has a full length approximately equal to DP 18–21 or the length of B1 chains.³⁰ Therefore, starch with a higher proportion of B1 chains could have a more perfect crystalline structure, and consequently, a higher T_o .²⁹ However, this rationale probably could not be applied to high-amylose starches. High-amylose corn starches had higher T_o but lower proportions of B1 chains compared with waxy corn or common corn starches (Table 4).

The T_o of starch could also be indirectly affected by the T_g (glass transition) of the surrounding amorphous regions because the crystalline lamellae would not begin to melt until the surrounding amorphous regions were

first melted.^{31,32} Slade and Levine³³ proposed that the high T_g of the amorphous regions in high-amylose corn starch was due to its large proportion of long amylopectin branches located in the amorphous lamellae. These chains formed association and decreased the mobility of the amorphous regions, thus resulting in elevated T_g . Because of the higher T_g in the amorphous regions, the crystalline lamellae would melt at a higher T_o for high-amylose corn starch. Shi and Seib²⁶ studied the difference in T_o among four waxy cereal starches and stressed the important indirect role of the amorphous regions surrounding the crystalline lamellae on T_o . The starch with the largest proportion of B1 chains had the highest T_o because the larger amount of B1 chains corresponded to increased interconnected, non-crystalline branched regions next to crystallites. This would cause a decrease in the mobility of chain segments in the amorphous regions, and consequently an increase in T_g . On the other hand, ΔH_g usually relates to the amount of double-helical structure in the crystalline lamellae.³⁴ We propose that the double-helical structure present in the amorphous lamellae from the co-crystallized long amylopectin chains or amylose molecules could also directly contribute to the overall ΔH_g .

The changes in T_o and ΔH_g of the unmodified and oxidized corn starches in this study confirmed our

Table 5. Gelatinization properties of unmodified and hypochlorite-oxidized corn starches^a

Starch	Oxidation level (% NaOCl)	Gelatinization temperature			Gelatinization enthalpy (J/g)
		Onset (°C)	Peak (°C)	End (°C)	
Waxy corn	Unmodified	68.4 ± 0.1	74.3 ± 0.1	81.6 ± 0.1	16.05 ± 0.06
	0.8	67.4 ± 0.2	73.6 ± 0.0	80.8 ± 0.1	16.03 ± 0.17
	2	67.4 ± 0.2	73.6 ± 0.0	81.61 ± 0.3	15.57 ± 0.22
	5	60.0 ± 0.2	68.1 ± 0.2	80.3 ± 0.1	14.14 ± 0.12
Common corn	Unmodified	69.4 ± 0.1	73.2 ± 0.1	78.4 ± 0.2	13.83 ± 0.14
		(94.2 ± 0.1) ^b	(100.4 ± 0.2)	(107.1 ± 0.0)	(1.65) ± 0.09
	0.8	69.2 ± 0.2	73.6 ± 0.1	79.1 ± 0.3	13.77 ± 0.18
		(92.1 ± 0.1)	(100.4 ± 0.1)	(107.9 ± 0.1)	(1.47 ± 0.20)
	2	69.1 ± 0.0	74.2 ± 0.0	80.9 ± 0.0	13.80 ± 0.04
		(93.6 ± 0.5)	(103.6 ± 0.0)	(108.0 ± 0.0)	(0.98 ± 0.16)
	5	64.9 ± 0.0	70.5 ± 0.1	78.0 ± 0.1	12.74 ± 0.05
		(92.4 ± 0.0)	(100.4 ± 0.1)	(106.3 ± 0.1)	(0.44 ± 0.10)
50% Amylose corn	Unmodified	69.3 ± 0.2	77.9 ± 0.0	106.6 ± 0.4	12.28 ± 0.20
	0.8	69.1 ± 0.2	76.8 ± 0.2	106.5 ± 0.2	10.57 ± 0.14
	2	67.7 ± 0.3	74.7 ± 0.7	106.1 ± 1.0	10.06 ± 0.29
	5	62.3 ± 0.2	71.5 ± 0.3	101.9 ± 0.4	10.67 ± 0.27
70% Amylose corn	Unmodified	69.8 ± 0.8	97.1 ± 0.8	107.5 ± 0.7	9.94 ± 0.54
	0.8	68.7 ± 0.2	100.4 ± 0.0	109.1 ± 0.0	9.35 ± 0.26
	2	70.3 ± 0.2	100.3 ± 0.2	108.8 ± 0.3	8.33 ± 0.48
	5	67.2 ± 0.6	72.6 ± 0.4	106.1 ± 0.3	8.06 ± 0.40

^a The data were averages of two measurements with standard deviations.^b Amylose–lipid complex peak.

proposed mechanism of structure degradation in the different oxidized corn starches. For WC, the degradation took place only at B2 and B3+ chains in the amorphous lamellae at 0.8% NaOCl level. The T_g of the amorphous lamellae was reduced; hence, the T_o was decreased (Table 5). Moreover, the crystalline structure was still intact; therefore, the ΔH_g of 0.8% NaOCl-oxidized WC was not significantly changed. At 2% NaOCl oxidation level, the crystalline lamellae began to degrade, probably from the edge; therefore, its ΔH_g slightly decreased from 16.1 to 15.6 J/g. At 5% NaOCl oxidation level, both T_o and ΔH_g significantly decreased, indicating further degradation of the double-helical structure in the crystalline lamellae. The decrease in T_o and ΔH was not significant until the 5% NaOCl level for CC was reached. The decrease in melting of the amylose–lipid complex in CC was faster than amylopectin melting (Table 5 and Fig. 7). These results support the previous findings that oxidation occurred on the amylose or lipid prior to reaction on the amylopectin long chains in the amorphous lamellae. The 70% AMC followed similar changes in both T_o and ΔH_g as in CC, but the extent of changes was smaller. The ΔH_g of 70% AMC included melting of the crystalline structures from amylopectin and from the amylose–lipid complexes. The decrease in ΔH_g was mainly ascribed to a decrease in the amount of amylose–lipid complex rather than amylopectin crystalline structure according to their thermograms (Fig. 7). NaOCl was preferentially consumed for the oxidation of lipids and amylose over amylopectin chains. The changes in T_o and ΔH_g of 50% AMC were different from

those of the others. A significant decrease in the ΔH_g , but not in the T_o , of 50% AMC was noted at the 0.8% NaOCl level (Table 5). The T_o of 50% AMC continued to decrease, while its ΔH_g remained unchanged with further increase in NaOCl level. The significantly lower ΔH_g at 0.8% NaOCl is proposed to result from the degradation of the amylose–lipid complex. This result again suggests a larger amount of amylose–lipid complex present in 50% AMC, and supports the previous results of faster degradation of amylose in 50% AMC than in 70% AMC (Fig. 2). The intermolecular amylose crystallites in 70% AMC might protect the amylose–lipid complex from oxidative degradation. A portion of amylose in 50% AMC may co-crystallize with amylopectin chains in the crystalline lamellae, which interconnected the crystalline and the amorphous lamellae. Once the amylose in this interconnecting structure in the amorphous lamellae was degraded, the amylopectin chains in the crystalline lamellae became less constrained and more mobile, thus resulting in significantly decreased T_o . Because the crystalline lamellae were still intact in oxidized 50% AMC, its ΔH_g did not change over the range of 0.8–5% NaOCl.

2.6. Retrogradation properties

DSC data of retrograded, unmodified and oxidized corn starches at 4 °C for 14 days are summarized in Table 6, and their thermograms are presented in Figure 8. In general, the retrogradation enthalpy (ΔH_r) slightly increased with increasing levels of oxidation. The extent

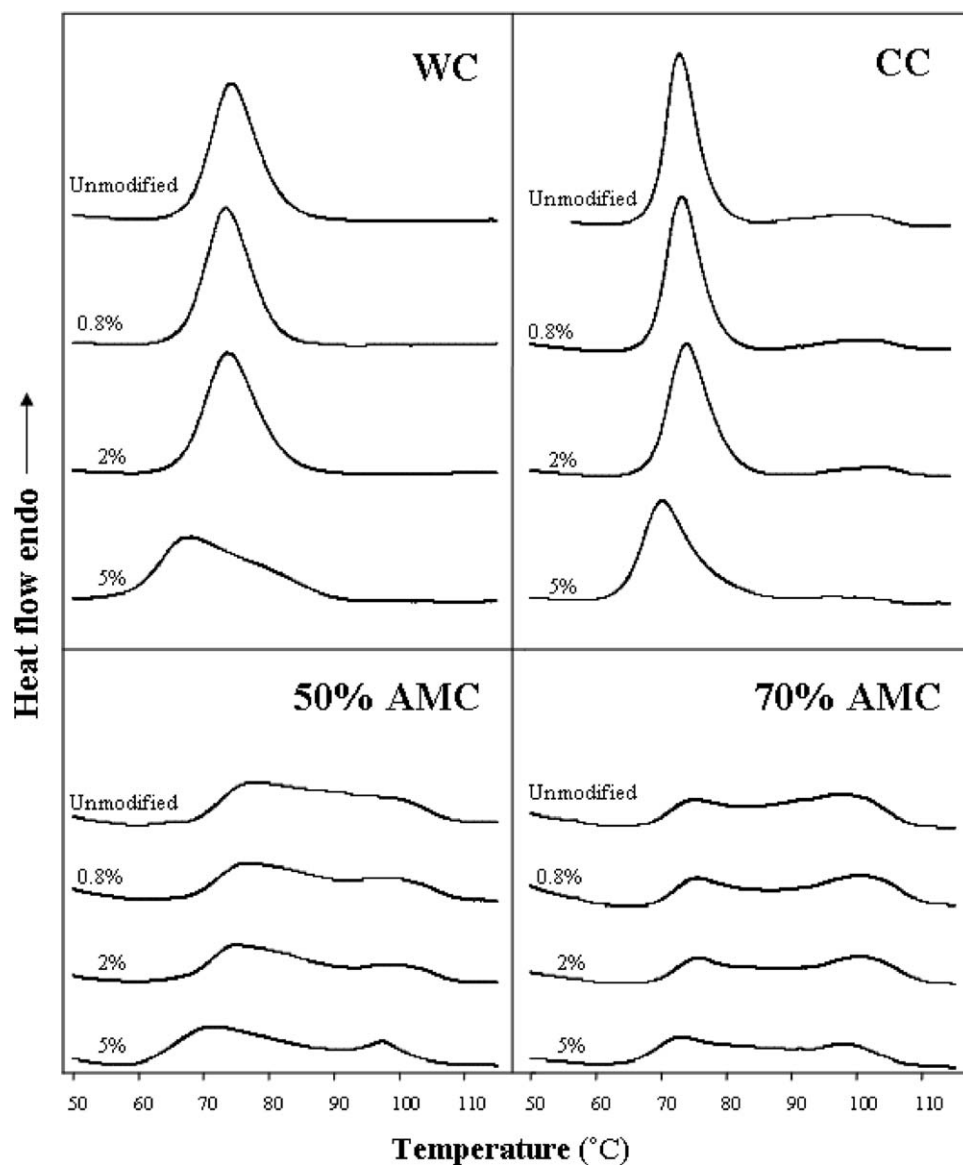


Figure 7. DSC thermograms of gelatinization of unmodified and hypochlorite-oxidized corn starches. The number next to each curve represents the NaOCl level.

of the increase in retrogradation enthalpy followed the order of $CC > 50\% AMC > WC > 70\% AMC$. Shi and Seib^{26,27} studied the relationship between the fine structure of amylopectin and their retrogradation of different cereal starches. They concluded that A and B1 chains predominantly controlled amylopectin retrogradation. With a larger proportion of B1 chains and a smaller proportion of A chains, a higher degree of amylopectin retrogradation was observed. This was attributed to the fact that the full length of a single cluster is equal to the length of the B1 chains.²⁹ Therefore, the B1 chains might be able to retrograde to the most perfect crystalline structure among amylopectin chains. On the other hand, the short A chains might hinder the reassociation of B1 chains and cause defects in the crystallites.^{35,36}

Oxidation could affect the retrogradation of starch molecules in two different mechanisms, increasing or decreasing. The degradation of B2 and B3+ amylopectin chains or even amylose molecules in the amorphous lamellae produced dextrans that might have the same length as B1 chains and behave like B1 chains. Hence, the amount of amylopectin crystallites or probably the co-crystallites between degraded amylose and amylopectin molecules increased, which would contribute to a higher ΔH_r . On the contrary, the formation of carboxyl or carbonyl groups on oxidized starch molecules would hinder the chain association, resulting in a lower ΔH_r . The increasing effect seemed to outweigh the decreasing effect for the retrogradation according to the increased ΔH_r for all corn starches. Most of the carboxyl groups

Table 6. Retrogradation properties of unmodified and hypochlorite-oxidized starches^a

Starch	% NaOCl	Retrogradation temperature			Retrogradation enthalpy (J/g)
		Onset (°C)	Peak (°C)	End (°C)	
Waxy corn	Unmodified	44.6 ± 0.2	57.6 ± 0.1	68.7 ± 0.3	7.36 ± 0.03
	0.8	43.8 ± 0.3	55.6 ± 0.0	65.8 ± 0.2	7.54 ± 0.12
	2	45.2 ± 0.3	57.3 ± 0.1	67.7 ± 0.5	7.52 ± 0.03
	5	45.4 ± 0.2	57.6 ± 0.2	67.7 ± 0.2	7.62 ± 0.12
Common corn	Unmodified	44.4 ± 0.1	54.5 ± 0.5	65.8 ± 0.2	6.82 ± 0.15
		(92.3 ± 0.2) ^b	(100.4 ± 0.2)	(106.9 ± 0.3)	(1.58 ± 0.15)
	0.8	43.5 ± 0.3	54.5 ± 0.0	65.5 ± 0.6	7.07 ± 0.04
		(92.5 ± 0.6)	(100.4 ± 0.0)	(107.8 ± 0.2)	(1.47 ± 0.08)
	2	44.6 ± 0.7	54.4 ± 0.0	64.2 ± 0.2	7.59 ± 0.04
		(93.2 ± 1.0)	(97.2 ± 0.7)	(107.8 ± 0.2)	(0.95 ± 0.52)
	5	45.0 ± 0.1	55.6 ± 0.0	67.1 ± 0.2	7.79 ± 0.10
		(93.1 ± 0.0)	(97.2 ± 0.7)	(107.1 ± 0.9)	(0.68 ± 0.26)
50% Amylose corn	Unmodified	45.9 ± 0.2	57.2 ± 0.9	78.7 ± 0.1	2.09 ± 0.08
		(90.0 ± 0.1)	(100.4 ± 0.2)	(107.7 ± 0.6)	(2.15 ± 0.07)
	0.8	50.9 ± 0.3	57.1 ± 0.0	80.8 ± 0.1	2.53 ± 0.13
		(91.8 ± 0.1)	(100.3 ± 0.0)	(108.5 ± 0.3)	(1.87 ± 0.01)
	2	46.7 ± 0.3	57.3 ± 0.2	80.9 ± 0.3	2.23 ± 0.10
		(90.3 ± 0.2)	(105.7 ± 0.4)	(111.8 ± 0.2)	(1.83 ± 0.06)
	5	46.5 ± 0.2	57.3 ± 0.3	81.0 ± 0.3	2.58 ± 0.07
		(94.5 ± 0.6)	(96.1 ± 0.2)	(98.7 ± 0.2)	(0.77 ± 0.09)
70% Amylose corn	Unmodified	47.2 ± 0.1	57.1 ± 0.9	59.1 ± 0.5	0.49 ± 0.15
		(88.7 ± 0.2)	(98.3 ± 0.0)	(106.9 ± 0.2)	(2.85 ± 0.01)
	0.8	49.9 ± 0.1	57.1 ± 0.1	59.0 ± 0.2	0.55 ± 0.03
		(89.7 ± 0.3)	(97.2 ± 0.5)	(107.9 ± 0.3)	(2.89 ± 0.42)
	2	47.1 ± 0.2	57.1 ± 0.3	74.9 ± 0.2	0.62 ± 0.03
		(86.9 ± 0.6)	(95.0 ± 0.5)	(106.6 ± 0.9)	(2.52 ± 0.14)
	5	44.9 ± 0.1	57.0 ± 0.4	63.2 ± 0.3	0.60 ± 0.14
		(87.8 ± 0.1)	(95.1 ± 0.1)	(99.1 ± 0.2)	(2.29 ± 0.09)

^a The data are averages of two measurements with standard deviation.^b Amylose–lipid complex peak.

were possibly formed close to the branching point of A and B1 chains, and the previous results showed that amylose was more prone to degradation than to forming carboxyl groups; therefore, they were not very effective in preventing the recrystallization of the chains. Oxidized WC contained a larger number of carboxyl groups (Table 1), and the A and B1 chains in the crystalline lamellae might also be partly degraded at the 5% NaOCl oxidation level (Table 2). Therefore, the increase in retrogradation with increasing NaOCl was lower for oxidized WC than for oxidized CC and 50% AMC. Because both amylose and amylopectin of 70% AMC degraded the least during oxidation (Fig. 2 and Table 2), a limited number of B1 chains were produced. As a result, 70% AMC exhibited the lowest extent of increase in retrogradation after oxidation. At 5% NaOCl oxidation, the amylose and amylopectin chains of 50% AMC degraded to a lower extent than those of CC; therefore, the long linear amylose chain in oxidized 50% AMC might hinder the retrogradation of starch molecules. Consequently, oxidized CC would have a larger increase in retrogradation than oxidized 50% AMC. The much lower ΔH_r in 50% and 70% AMCs was attributed to their smaller numbers of amylopectin B1 chains and

larger amounts of amylose, which was difficult to reassociate into crystalline structure due to its large DP.

When the ΔH_g and ΔH_r of the amylose–lipid complex in native and oxidized CC were compared, it was found that the residual amylose–lipid complex after oxidation fully reassociated after gelatinization as shown by their similar values. This result suggests that the portion of amylose–lipid complex modified by oxidation, which could be on amylose or lipids or both, could not reassociate and did not contribute to the ΔH_r . Based on this assumption, the ΔH_r of the amylose–lipid complex corresponded to its amount in native and oxidized 50% and 70% AMCs. The amount of amylose–lipid complex decreased the most in 50% AMC and the least in 70% AMC. Unlike CC or 50% AMC, the amylose–lipid complex in 70% AMC was probably protected by co-crystallized amylose–amylopectin or amylose–amylose and did not greatly change even after oxidation with 5% NaOCl.

2.7. Pasting properties

Pasting viscosity profiles of unmodified and oxidized corn starches by a Micro ViscoAmylograph are shown

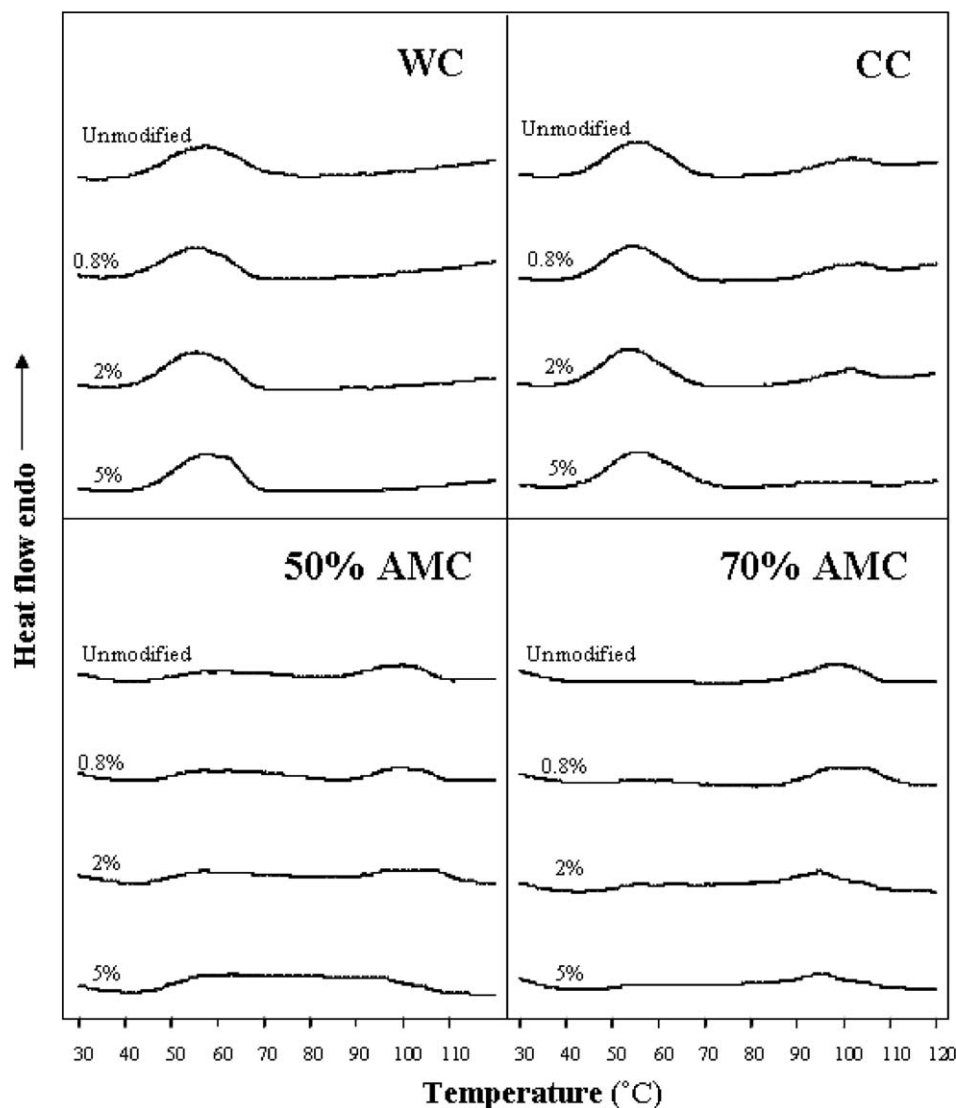


Figure 8. DSC thermograms of retrogradation of unmodified and hypochlorite-oxidized corn starches. The number next to each curve represents the NaOCl level.

in Figure 9. Oxidation generally decreased the pasting temperature of all corn starches, particularly at the 5% NaOCl level.^{12,20} The decrease in pasting temperature was attributed to the depolymerization of starch structure, resulting in a weakened granule organization. WC did not show a significant decrease in pasting temperature until the 5% NaOCl level was reached. Amylopectin contributes to starch swelling, whereas amylose and lipids restrict the swelling,³⁷ and starch with a higher amylose content tends to have a higher pasting temperature. According to the previous results, oxidation first occurred to the amorphous lamellae where most amylose is located, and amylose was more susceptible to depolymerization than the amylopectin B2 and B3+ chains. The degraded amylose exerted less inhibitory constraint on starch swelling; therefore, the pasting temperatures of oxidized starches decreased. Because of the

absence of amylose, the pasting temperature of WC did not change after oxidation until the 5% NaOCl level. The decrease in the pasting temperature of oxidized WC at 5% NaOCl was assumed to result from degradation of its crystalline lamellae.

WC and CC displayed increased peak and final viscosities and less breakdown after 0.8% NaOCl oxidation, which has been reported previously.^{12,20,38} This phenomenon was attributed to the formation of hemiacetal or hemiketal cross-links from oxidation, which are assumed to occur mostly among amylopectin molecules and to a lesser extent between amylopectin and amylose molecules.³⁹ These cross-links could stabilize the swollen granules and overcome the negative impacts from minor depolymerization. This cross-linking effect was still observed in CC but not in WC after 2% NaOCl oxidation. This finding supports previous results that the crystalline

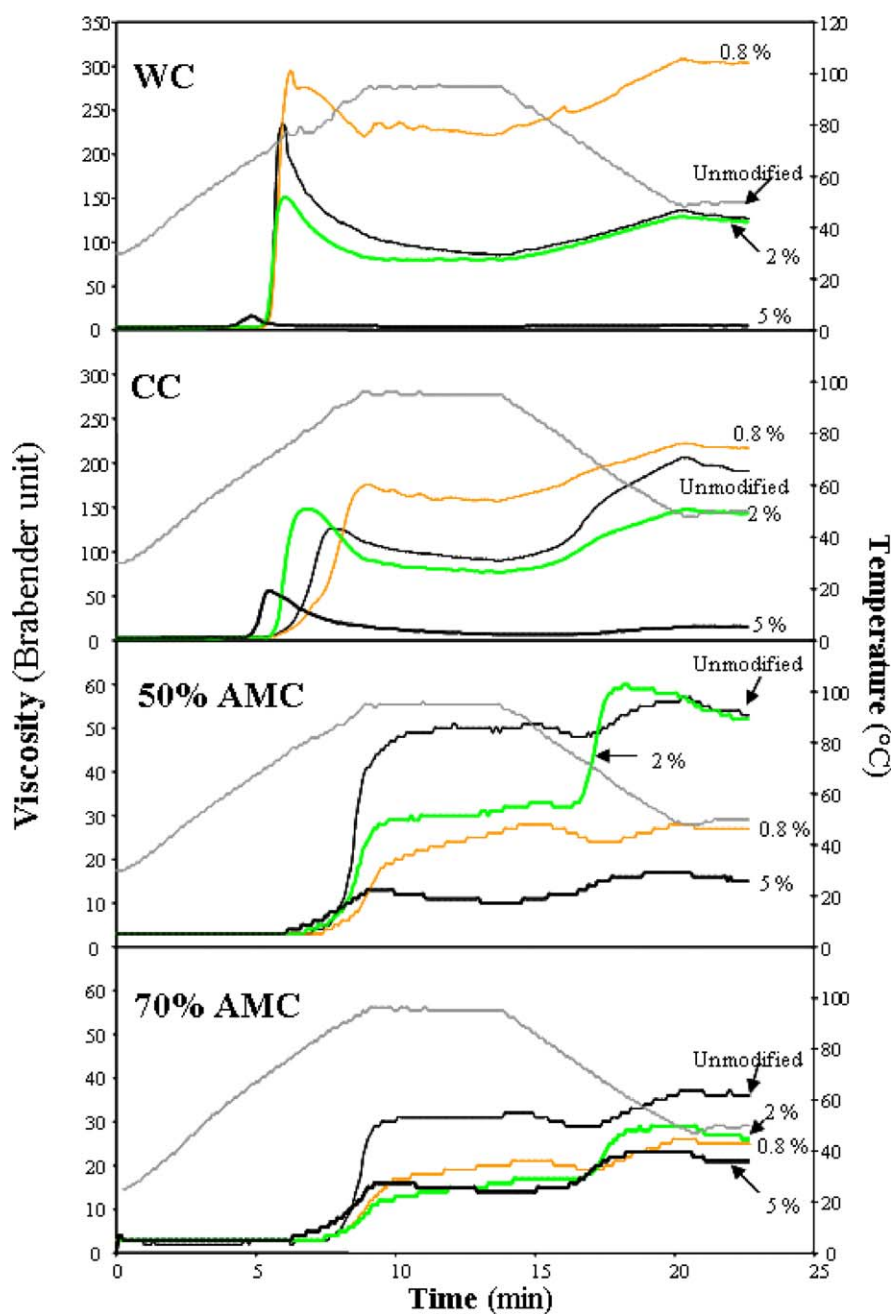


Figure 9. Pasting profiles of unmodified and hypochlorite-oxidized corn starches by a Micro ViscoAmylograph. The number next to each curve represents the NaOCl level.

lamellae of WC started to degrade at the 2% NaOCl oxidation level; therefore, excessive depolymerization prevailed over the cross-linking effect. However, the 2% NaOCl-oxidized CC had more breakdown and less setback than its unmodified counterpart, suggesting that amylose in CC could not form a strong gel network due to depolymerization. Although 50% and 70% AMCs contained a similar or higher carboxyl and carbonyl contents compared with CC at the 0.8% NaOCl level, the hemiacetal cross-linking effect was not noted. It might be possible that amylopectin in high AMCs

was interrupted by amylose and not located close to each other due to its limited amount. Therefore, it was physically unfavorable to form the hemiacetal or hemiketal cross-links. The setback of 50% and 70% AMCs at the 2% NaOCl level significantly increased in terms of rate and extent. It is possible that lipids were oxidized after 2% NaOCl oxidation; therefore, amylose reassociation was no longer hindered by the presence of lipids. When NaOCl was increased to 5%, amylose was likely excessively degraded, resulting in lower final and setback viscosities.

3. Experimental

3.1. Materials

Waxy corn (Cargill Gel 04230), common corn (Cargill Gel 03420), 50% high-amylose corn (AmyloGel 03001), and 70% high-amylose corn (AmyloGel 03003) starches were obtained from Cargill Food and Pharma Specialties North America (Cedar Rapids, IA, USA). *Pseudo-monas* isoamylase (EC 3.2.1.68) was purchased from Hayashibara Biochemical Laboratories, Inc. (Kayama, Japan). NaOCl containing 6% active chlorine was purchased from J. T. Baker Chemical Co. (Phillipsburg, NJ, USA). All other chemicals were of ACS grade. The moisture content of starches was determined according to AACC Method 44-15A.⁴⁰

3.2. Starch oxidation

The starch oxidation procedure followed the method of Autio et al.⁴¹ with modifications. A 40% (w/w) starch slurry (total weight of 1125 g) was prepared in a 2-L reaction vessel equipped with a heating mantle. The starch slurry was mechanically stirred and maintained at 35 °C, and the pH was adjusted to 9.5 with 2 M NaOH. Three levels of oxidation were achieved by slowly adding NaOCl, 60 g (0.8 g Cl/100 g starch, 0.8% w/w), or 150 g (2 g Cl/100 g starch, 2% w/w) or 375 g (5 g Cl/100 g starch, 5% w/w) into the starch slurry within 30 min while maintaining the pH at 9.5 with 1 M H₂SO₄ and a temperature of 35 °C. After the NaOCl addition, the starch slurry was maintained at the same pH and temperature for an additional 50 min with stirring. The slurry was then neutralized to pH 7.0 with 1 M H₂SO₄, filtered through suction (Whatman filter #4), washed with deionized water, and dried in an oven at 40 °C for 48 h. A portion of native and oxidized starches was defatted by refluxing with 85% (v/v) MeOH for 24 h.

3.3. Carboxyl content

The carboxyl content of oxidized starches was determined according to the modified procedure of Chattopadhyay et al.⁴ Starch (2 g) was mixed with 25 mL of 0.1 M HCl in a 150-mL beaker at room temperature with magnetic stirring for 30 min. The slurry was vacuum filtered through a 150-mL medium porosity fritted glass funnel, and a fine stream of deionized water from a wash bottle was used to quantitatively transfer the sample from the beaker. The sample was washed with 400 mL of deionized water in order to completely remove chloride ion. The starch cake was then quantitatively transferred to a 500-mL beaker with the aid of deionized water, and the slurry was diluted to approximately 300 mL. The starch slurry was heated in a boiling

water bath with continuous stirring for 15 min to ensure complete gelatinization. The hot starch solution was adjusted to approximately 450 mL with boiling deionized water and immediately titrated to pH 8.3 with standardized 0.01 M NaOH with stirring. The amount of 0.01 M NaOH used in milliliter was recorded. Unmodified starches were used as the blanks for oxidized starches to correct for inherent acidic substances. Instead of stirring with 0.1 M HCl, 2 g of unmodified starch was stirred with 25 mL of deionized water.

Carboxyl group content was calculated as follows:

$$\text{mequiv of acidity/100 g starch} = \frac{[(\text{Sample} - \text{Blank}) \text{ mL} \times \text{molarity of NaOH} \times 100]}{\text{Sample weight (db) in g}}$$

$$\text{Percentage of carboxyl content} = \frac{[\text{mequiv of acidity} / 100 \text{ g starch}] \times 0.045}{100 \text{ g starch}} \times 0.045$$

3.4. Carbonyl content

The carbonyl content of oxidized starches was determined by following the titrimetric method of Smith.⁴² Starch (4 g) was suspended in 100 mL of distilled water in a 500-mL flask. The suspension was gelatinized in a boiling water bath for 20 min, cooled to 40 °C, adjusted to pH 3.2 with 0.1 M HCl, and 15 mL of hydroxylamine reagent was added. The flask was stopped and placed in a 40 °C water bath for 4 h with slow shaking. The excess hydroxylamine was determined by rapidly titrating the reaction mixture to pH 3.2 with standardized 0.1 M HCl. A blank determination with only hydroxylamine reagent was performed in the same manner. The hydroxylamine reagent was prepared by first dissolving 25 g of hydroxylamine hydrochloride in 100 mL of 0.5 M NaOH before the final volume was adjusted to 500 mL with distilled water. The carbonyl content was calculated as follows:

Percentage of carbonyl content =

$$\frac{[(\text{Blank} - \text{Sample}) \text{ mL} \times \text{Acid molarity} \times 0.028 \times 100]}{\text{Sample weight (db) in g}}$$

3.5. Characterization of starch structures

The carbohydrate profiles of native and oxidized starches were determined by a high-performance size-exclusion chromatography (HPSEC) system (Waters Corporation, Milford, MA). Defatted starch (80 mg) was solubilized by heating and stirring in 5 mL of 0.2 M NaOH at 65 °C for 18 h. The starch solution was neutralized with 1 M HCl and shortly boiled on a heating coil. The solubilized starch was precipitated with 50 mL of MeOH at room temperature for 24 h. The precipitated starch was collected by centrifugation at 1520g

for 15 min, washed with 30 mL of MeOH, and dried at 40 °C for 24 h. The dried starch (9 mg) was stirred in 3.2 mL of deionized water, heated in boiling water for 30 min, and then centrifuged at 4500g for 5 min. The supernatant was injected into the HPSEC system consisting of a 515 HPLC pump with an injector with a 100- μ L sample loop, an in-line degasser, a series Shodex OHpak columns (KB guard column, analytical columns KB-802, and KB-804) maintained at 55 °C and a 2410 refractive index detector maintained at 40 °C. The eluent was 0.1 M NaOAc and 0.02% NaN₃ solution with a flow rate of 0.7 mL/min.

3.6. Isolation of amylopectin from starch samples

The method of amylopectin isolation from native and oxidized starch samples was modified from the procedure of Takeda et al.⁴³ Approximately 200 mg of defatted starch was dissolved in 12 mL of 0.2 M NaOH at 65 °C with magnetic stirring in a 25-mL capped test tube for 18 h to achieve complete dissolution. The starch solution was then adjusted to pH of 6.8–7.0 with 1 M HCl, added with 2.4 mL of *n*-BuOH, flushed with nitrogen gas for 30 s, capped and stirred at ~100 °C for 3 h. The heated starch mixture was gradually cooled to room temperature over 24 h by immersing the sample test tube in a sealed 2-L dewar flask (Thermo-flask, Lab-line instruments Inc., Melrose Park, IL, USA) filled with hot water to allow the formation of the amylose–*n*-BuOH complex. The cooled starch mixture was stored at 4 °C for 48 h. The amylose–*n*-BuOH complex was removed by centrifugation at 12,100g and 4 °C for 45 min. The supernatant containing mostly amylopectin was further purified for another recrystallization cycle with the addition of 1 mL of *n*-BuOH. Finally, the purified amylopectin in the supernatant was recovered by precipitating with 100 mL of MeOH at room temperature for 24 h, centrifuging at 1520g for 15 min, washing with 30 mL of MeOH, and drying at 40 °C for 24 h.

3.7. Chain-length distribution of amylopectin

The chain-length distribution of amylopectin was characterized by high-performance anion-exchange chromatography using a pulsed amperometric detector (HPAEC-PAD) according to the method of Kasemsuwan et al.⁴⁴ with modification in sample preparation. The HPAEC-PAD (DX500, Dionex Co., Sunnyvale, CA, USA) system consisted of the following components: GP50 gradient pump, LC20-1 chromatography organizer, ED40 electrochemical detector, 4 \times 50-mm CarboPac PA1 guard column, 4 \times 250-mm CarboPac PA1 analytical column, and AS40 automated sampler. An amylopectin solution containing 9 mg of purified amylopectin in 3.2 mL of deionized water was heated in a boiling water bath with stirring for 1 h. After

cooling to room temperature, 0.4 mL of 0.1 M acetate buffer of pH 3.5 was added and thoroughly mixed before adding *Pseudomonas* isoamylase (1770 U). The mixture was incubated in a water bath shaker at 40 °C for 48 h to allow for the enzymatic debranching. The enzyme was inactivated by heating the mixture in a boiling water bath for 20 min, and the mixture was centrifuged at 4500g for 5 min. The supernatant was placed into sample vials for injection.

3.8. Ion-exchange chromatography

Oxidized starch was separated into anionic and non-anionic dextrin fractions by following the anion-exchange chromatography method of Zhu et al.²³ with modifications. Defatted oxidized starch (80 mg) was heated in 5 mL of 0.2 M NaOH with stirring in a 25-mL capped test tube at 65 °C for 18 h in an oil bath to achieve complete dissolution. The starch solution was neutralized with 1 M HCl and shortly boiled with a heating coil. The hot starch solution was centrifuged at 4500g for 5 min. The supernatant was then injected into an anion-exchange column (C Column, 1.6 cm \times 20 cm), which was packed with 30 mL of DEAE Sepharose fast-flow gel and equilibrated with 0.005 M Bis Tris buffer at pH 6.5 (Amersham Bioscience Corp, Piscataway, NJ, USA). The non-anionic dextrans were eluted with 0.005 M Bis Tris buffer at 0.5 mL/min in a descending order and collected the first 60 mL of eluent. The eluent was concentrated to approximately 10 mL by transferring the eluent into a glass tray (30 cm \times 18 cm \times 2.5 cm) and heated at 40 °C in a forced-air oven for 5 h. The bound anionic dextrans were subsequently eluted with 0.5 M KOH at 0.5 mL/min in a descending order to collect a total amount of 500 mL of the eluent. The bound fraction was neutralized with 1 M HCl and concentrated to approximately 150 mL by the same method described above. The dextrans in both fractions were precipitated with 10-fold MeOH of the eluent volume and then kept at room temperature for 24 h. The precipitated dextrans were recovered by centrifugation at 1520g for 15 min, washed with 30 mL of MeOH, and dried at 40 °C for 24 h. The carbohydrate structure profile and amylopectin chain-length distribution of the fractionated dextrans were characterized by following the method previously described.

3.9. X-ray diffraction crystallinity

The X-ray diffraction patterns of starches were obtained with a copper anode X-ray tube using a Philips Analytical diffractometer (Philips, Almelo, The Netherlands). The diffractometer was operated at 27 mA and 50 kV. The scanning region of the diffraction angle (2θ) was from 5° to 45° at 0.1° step size with a count time of 2 s. The starch samples were equilibrated in a 100% relative

humidity chamber for 24 h at room temperature before scanning. The X-ray diffraction pattern was printed on A4 paper. A straight line connecting between two points at the signal at 5° and 45° was drawn and considered as a baseline. A smooth curve line touching all the base points of each upper diffraction peak starting from 5° and 45° was also drawn and considered as a border line separating the crystalline and amorphous regions. The area above the border line was the crystalline region and the one under the line was the amorphous region. The total area and amorphous area were measured using a planimeter. The percent crystallinity was calculated as follows:

$$\% \text{ Crystallinity} = (\text{Total area} - \text{Amorphous area}) / \text{Total area} \times 100$$

3.10. Thermal properties

The thermal transition of starch samples was measured by a Pyris-1 differential scanning calorimeter (DSC, Perkin–Elmer, Norwalk, CT, USA). Starch (12 mg) was weighed into a stainless steel DSC pan (part number 03190029), and deionized water (24 µL) was added to obtain a starch to water ratio of approximately 1:2. The pan was hermetically sealed, equilibrated at room temperature for 24 h, and scanned from 25 to 140 °C at a rate of 10 °C/min. After scanning, the gelatinized sample was stored at 4 °C for 14 days and rescanned from 5 to 135 °C at a rate of 10 °C/min. The characteristics of the transitions, including onset (T_o), peak (T_p), and end (T_e) temperatures, and the enthalpy of gelatinization (ΔH_g) and retrogradation (ΔH_r) were calculated (Pyris Software for Windows version 3.81, Perkin–Elmer) based on starch dry mass. The instrument was calibrated with indium, and an empty pan was used as the reference.

3.11. Pasting properties

The pasting properties of native and oxidized starches (10%, w/w, d.b.) were determined with a Micro Visco-AmyloGraph (C.W. Brabender Instruments, Inc., South Hackensack, NJ) operated at a speed of 250 rpm and a 300-cm g cartridge. The starch slurry was heated from 50 to 95 °C at a programmed rate of 4.5 °C/min, held at 95 °C for 5 min, and cooled to 50 °C at 4.5 °C/min.

3.12. Experimental design and statistical analyses

A 4 × 4 completely randomized design (CRD) structure (four starch types and four hypochlorite levels, 0%, 0.8%, 2%, and 5%) was used. Each combination was performed in duplicate. The data were statistically analyzed by the SAS program (SAS 1986). General linear

model procedure (GLM) was conducted to identify differences among data. All significant differences were reported at the 95% confidence interval.

Acknowledgements

We would really like to thank Dr. P. Tomasik from the Agricultural University of Cracow, Cracow, Poland, Dr. P. A. Seib from Grain Science Department, Kansas State University, KS, USA, and Dr. W. Praznik from the University of Natural Resources and Applied Life Science, Vienna, Austria for their support, discussions and recommendations. Without their kind assistance, this work would never have been accomplished.

References

1. Production and use of hypochlorite-oxidized starches by Scallet, B. L.; Sowell, E. A. In *Starch Chemistry and Technology*; Whistler, R. L., Paschall, E. F., Eds.; Academic Press: New York, 1967; Vol. 2, pp 237–251.
2. Konoo, S.; Ogawa, H.; Mizuno, H.; Iso, N. *Jpn. Soc. Food Sci. Technol.* **1996**, *43*, 880–886.
3. Mazur, P. Y.; Stolyarova, L. I.; Muraschkina, L. V.; Dyatlov, V. A. *Emahrung* **1989**, *13*, 155–156.
4. Chattopadhyay, S.; Singhal, R. S.; Kulkarni, P. R. *Carbohydr. Polym.* **1997**, *34*, 203–212.
5. Converted starches by Wurzburg, O. B. In *Modified Starches: Properties and Uses*; Wurzburg, O. B., Ed.; CRC Press: Boca Raton, 1986; pp 18–38.
6. Hullinger, C. H.; Whistler, R. L. *Cereal Chem.* **1951**, *28*, 153–157.
7. Whistler, R. L.; Linke, E. G.; Kazeniae, S. *J. Am. Chem. Soc.* **1956**, *78*, 4704–4709.
8. Whistler, R. L.; Schweiger, R. *J. Am. Chem. Soc.* **1957**, *79*, 6460–6464.
9. Schmorak, J.; Meizler, D.; Lewin, M. *Starch/Stärke* **1962**, *14*, 278–290.
10. Potze, J.; Hiemstra, P. *Starch/Stärke* **1963**, *15*, 217–225.
11. Hebeish, A.; El-Thalouth, I. A.; Refai, R.; Ragheb, A. *Starch/Stärke* **1989**, *41*, 293–298.
12. Kuakpetoon, D.; Wang, Y.-J. *Starch/Stärke* **2001**, *53*, 211–218.
13. Wu, H. C. H.; Sarko, A. *Carbohydr. Res.* **1978**, *61*, 7–25, 27–40.
14. Imberty, A.; Perez, S. *Biopolymers* **1988**, *27*, 1205–1221.
15. Hizukuri, S.; Kaneko, T.; Takeda, Y. *Biochim. Biophys. Acta* **1983**, *760*, 188–191.
16. Hizukuri, S. *Carbohydr. Res.* **1985**, *141*, 295–306.
17. Jenkins, P. J.; Donald, A. M. *Int. J. Biol. Macromol.* **1995**, *17*, 315–321.
18. Mellies, R. L.; Mehlretter, C. L.; Senti, F. R. *J. Chem. Eng. Data* **1960**, *5*, 169–171.
19. Prey, V.; Siklossy, St. *Starch/Stärke* **1971**, *23*, 235–238.
20. Wang, Y.-J.; Wang, L. *Carbohydr. Polym.* **2003**, *52*, 207–217.
21. Hanashiro, I.; Abe, J.-I.; Hizukuri, S. *Carbohydr. Res.* **1996**, *283*, 151–159.
22. Hizukuri, S. *Carbohydr. Res.* **1986**, *147*, 342–347.

23. Zhu, Q.; Sjöholm, R.; Nurmi, K.; Bertoft, E. *Carbohydr. Res.* **1998**, *309*, 213–218.
24. Asaoka, M.; Okuno, K.; Fuwa, H. *Agric. Biol. Chem.* **1985**, *49*, 373–379.
25. Jane, J.; Shen, L.; Lim, S.; Kasemsuwan, T.; Nip, W. K. *Cereal Chem.* **1992**, *69*, 528–535.
26. Shi, Y. C.; Seib, P. A. *Carbohydr. Res.* **1992**, *227*, 131–145.
27. Shi, Y. C.; Seib, P. A. *Carbohydr. Polym.* **1995**, *26*, 141–147.
28. Yuan, R. C.; Thompson, D. B.; Boyer, C. D. *Cereal Chem.* **1993**, *70*, 81–89.
29. Jane, J.; Chen, Y. Y.; Lee, L. F.; McPherson, A. E.; Wong, K. S.; Radosavljevic, M.; Kasemsuwan, T. *Cereal Chem.* **1999**, *76*, 629–637.
30. Cameron, R. E.; Donald, A. M. *Polymer* **1992**, *33*, 2628–2635.
31. Donovan, J. W. *Biopolymers* **1979**, *18*, 263–275.
32. Donovan, J. W.; Mapes, C. J. *Starch/Stärke* **1980**, *32*, 190–193.
33. Slade, L.; Levine, H. *Carbohydr. Polym.* **1988**, *8*, 183–208.
34. Cooke, D.; Gidley, M. J. *Carbohydr. Res.* **1992**, *227*, 103–112.
35. Krusi, H.; Neukom, H. *Starch/Stärke* **1984**, *36*, 300–305.
36. Levine, H.; Slade, L. *Carbohydr. Polym.* **1986**, *6*, 213–244.
37. Tester, R. F.; Morrison, W. R. *Cereal Chem.* **1990**, *67*, 551–557.
38. Farley, F. F.; Hixon, R. M. *Eng. Chem. Ind.* **1942**, *34*, 667–681.
39. Seib, P. A. Principles of starch modification. Agricultural Experiment Station at Kansas State University: Manhattan, KS, 1997; Contribution No. 97-480-A.
40. Method 44-15A by American Association of Cereal Chemists. In *Approved Methods of AACC*, 9th ed., 1995.
41. Autio, K.; Suortti, T.; Hamunen, A.; Poutanen, K. *Carbohydr. Polym.* **1996**, *29*, 155–161.
42. Characterization and analysis of starches by Smith, R. J. In *Starch Chemistry and Technology*; Whistler, R. L., Paschall, E. F., Eds.; Academic Press: New York, 1967; Vol. 2, pp 620–625.
43. Takeda, Y.; Hizukuri, S.; Juliano, B. O. *Carbohydr. Res.* **1986**, *148*, 299–308.
44. Kasemsuwan, T.; Jane, J.-L.; Schnable, P.; Stinard, P.; Robertson, D. *Cereal Chem.* **1995**, *72*, 457–464.